Calculation of the nucleon-nucleon interaction due to vector-meson exchange

L. S. Celenza, C. M. Shakin, and Wei-Dong Sun
Department of Physics and Center for Nuclear Theory, Brooklyn College of the City University of New York, Brooklyn, New York 11210
(Received 15 January 1996)

We make use of a momentum-space bosonization of a generalized Nambu–Jona-Lasinio model to calculate the contribution of rho and omega exchange to the one-boson-exchange (OBE) model of the nucleon-nucleon interaction. Momentum-dependent meson-quark coupling constants are obtained in the bosonization scheme. A vector-meson-dominance (VMD) model is used to obtain information concerning the momentum dependence of the meson-nucleon vertex, other than that which arises from the momentum dependence of the meson-quark coupling constants. We find good agreement with the magnitude of the force at $q^2=0$ for both rho and omega exchange. The momentum dependence of the interaction in the region $-0.2\ \mathrm{GeV}^2 \leq q^2 \leq 0$ was calculated. We only obtain about two-thirds of the strength of the OBE interaction at $q^2=-0.2\ \mathrm{GeV}^2$, suggesting the importance of interactions of shorter range than that considered here. (We note that, for $-0.2\ \mathrm{GeV}^2 \leq q^2 \leq 0$, we span the range of q^2 of significance for nuclear structure studies.) [S0556-2813(96)00408-6]

PACS number(s): 13.75.Cs, 12.40.Vv, 21.30.Fe, 24.85.+p

I. INTRODUCTION

The parametrization of the nucleon-nucleon potential as given by the one-boson-exchange (OBE) model [1] is extremely useful for nuclear structure studies and provides the basis for the calculation of the properties of nuclear matter in relativistic-Brueckner-Hartree-Fock theory [2]. The OBE potentials of Ref. [1] have been extensively applied in the study of the properties of nuclear matter and finite nuclei. In the relativistic-Brueckner-Hartree-Fock theory, one finds good values for the nuclear saturation density and binding energy. One is also able to reproduce the strength of the large (Lorentz) scalar and vector potentials that are used in Dirac phenomenology to within a few percent. However, the relation of the OBE model to more fundamental models of the strong interaction has not been understood. We have undertaken a program to study the OBE model, making use of a bosonized version of an extended Nambu–Jona-Lasinio (NJL) model [3,4]. (It is necessary to extend the NJL model to include a description of confinement in order to calculate the properties of the rho and omega mesons. Such a generalization of the NJL model has been given in our earlier work [5,6].)

In our work we make use of a Lagrangian describing the interaction of up and down quarks,

$$\mathcal{L}(x)=\overline{q(x)}(i\partial\!\!\!/-m_q^0)q(x)+\frac{G_S}{2}\left[(\overline{qq})^2+(\overline{qi}\gamma_5\vec{\tau}q)^2\right]$$
$$-\frac{G_V}{2}\left[(\overline{q}\gamma^\mu\vec{\tau}q)^2+(\overline{q}\gamma_5\gamma^\mu\vec{\tau}q)^2\right]-\frac{G_\omega}{2}(\overline{q}\gamma^\mu q)^2$$
$$+\mathcal{L}_{\mathrm{conf}}(x), \tag{1.1}$$

where $\mathcal{L}_{\mathrm{conf}}(x)$ refers to our treatment of confinement. Here we will concentrate on the rho and omega mesons and will write G_ρ rather than G_V in the following. The treatment of confinement in our model has been discussed extensively elsewhere [5–7]. However, we will include a few comments relevant to our model of confinement in the next section.

The organization of our work is as follows. In Sec. II we will define some tensors that play an important role in the bosonization scheme and present two basic bosonization relations used to introduce the rho and omega mesons in the formalism. In Sec. III we review the phenomenological representation of isoscalar and isovector electromagnetic form factors of the nucleon. In Sec. IV we go on to provide a vector-meson-dominance (VMD) model of the nucleon electromagnetic form factors. Our model envisions a valence-quark ''core'' that is strongly coupled to various meson fields. In the VMD model, a photon couples to the rho and omega fields in the vicinity of the nucleon. The dipole form for the electromagnetic form factors then emerges from an interplay of the meson propagator, the core form factor and the momentum dependence of the meson-quark coupling constant. In Sec. IV we specify those core form factors that allow us to fit the isoscalar and isovector electromagnetic form factors of the nucleon using our VMD model. In Sec. V we make use of the core form factors to calculate the nucleon-nucleon interaction that arises from rho and omega exchange. (We point out that, although our results are generally satisfactory, there are a large number of diagrams that we have not considered. We believe these diagrams will give interactions of shorter range than the interactions we consider here. Therefore, we do not expect our model to work well for large values of $-q^2$.) Finally, in Sec. VI, we include some further discussion and conclusions.

II. MOMENTUM-SPACE BOSONIZATION OF THE NJL MODEL

In this section we review procedures used in the momentum-space bosonization of an extended NJL model for the quark-antiquark channels with the quantum numbers of the rho and omega mesons [7]. We will begin our discussion by defining the tensors

$$\hat{J}^{\mu\nu}_{(\rho)}(q)=-\tilde{g}^{\mu\nu}(q)\hat{J}_{(\rho)}(q^2), \tag{2.1}$$

$$\hat{J}^{\mu\nu}_{(\omega)}(q)=-\tilde{g}^{\mu\nu}(q)\hat{J}_{(\omega)}(q^2), \tag{2.2}$$

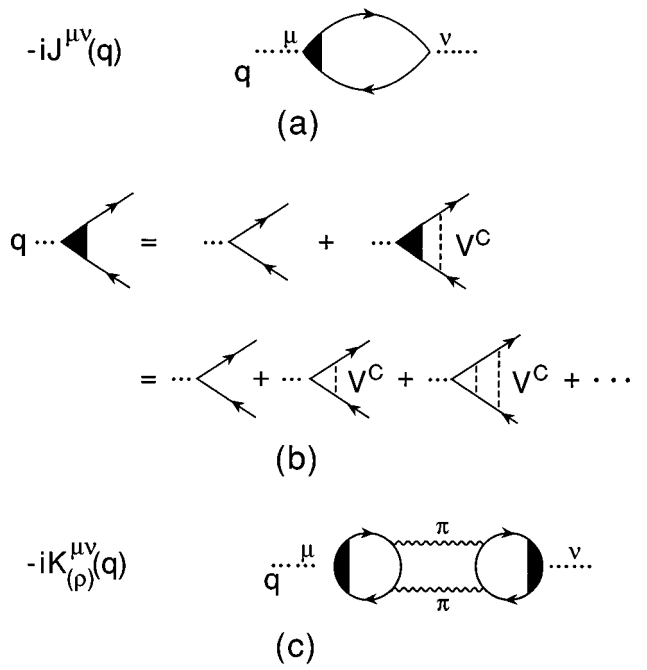

FIG. 1. (a) The basic quark-antiquark loop diagram of the NJL model is shown for the rho and omega channels. The solid triangular area denotes a vertex function for the confining interaction (a linear potential). (b) The equation that is solved to obtain the vertex operator for the confining potential, V^C, is shown. The driving term is γ^μ, or $\gamma^\mu\tau_3$, for the isoscalar and isovector channels, respectively. (c) Calculation of the diagram shown yields the tensor, $\hat{K}^{\mu\nu}_{(\rho)}(q)$, that describes the coupling of the vector-isovector channel to the two-pion continuum. For $q^2>4m_\pi^2$, $\hat{K}^{\mu\nu}_{(\rho)}(q)$ has an imaginary part that provides the width for the rho meson. We note that $m_\rho\Gamma_\rho(q^2)=g^2_{\rho qq}(q^2)\mathrm{Im}\,\hat{K}_{(\rho)}(q^2)$.

with $\tilde{g}^{\mu\nu}(q)=g^{\mu\nu}-q^\mu q^\nu/q^2$. Here the $\hat{J}^{\mu\nu}(q)$ represent quark-antiquark loop integrals obtained when evaluating the diagrams shown in Fig. 1 [7]. The carets over the symbols in Eqs. (2.1) and (2.2) indicate that we have included vertex functions in the calculation of $\hat{J}^{\mu\nu}(q)$ that sum a ladder of confining interactions [6]. These vertex functions are represented by solid triangular areas in Fig. 1.

For the case of the rho, it is particularly important to include the effects of coupling to the two-pion continuum. Thus, we define the tensor [7]

$$\hat{K}^{\mu\nu}_{(\rho)}(q)=-\tilde{g}^{\mu\nu}(q)\hat{K}_{(\rho)}(q^2). \tag{2.3}$$

(See Fig. 1.) For $q^2>4m_\pi^2$, $\hat{K}_{(\rho)}(q^2)$ has an imaginary part that gives rise to the rho width. Note that, because we have included a model of confinement, these various tensors have no quark-antiquark cuts in the complex q^2 plane. (The confining interaction prevents the quark and antiquark from going on-mass shell simultaneously.)

Bosonization may be achieved by considering a string of quark-antiquark interactions. For example, consider a scattering amplitude for a quark-antiquark pair with the quantum number of the rho meson. If we suppress reference to Dirac matrices and isospin matrices, we have

TABLE I. Values of $g_{\rho qq}(q^2)$ and $g_{\omega qq}(q^2)$ obtained in an earlier work [8] are presented.

q^2 (GeV^2)	$g_{\rho qq}(q^2)$	$g_{\omega qq}(q^2)$
0.7	2.66	2.80
0.6	2.82	2.98
0.5	2.98	3.14
0.4	3.13	3.30
0.3	3.27	3.45
0.2	3.41	3.59
0.1	3.54	3.73
0.0	3.66	3.86
−0.1	3.74	3.96
−0.2	3.81	4.04
−0.3	3.88	4.11
−0.4	3.92	4.16
−0.5	3.97	4.21
−0.6	4.01	4.25
−0.7	4.04	4.29
−0.8	4.07	4.32
−0.9	4.10	4.35
−1.0	4.12	4.38

$$T_{(\rho)}(q^2)=\frac{G_\rho}{1-G_\rho[\hat{J}_{(\rho)}(q^2)+\hat{K}_{(\rho)}(q^2)]}. \tag{2.4}$$

We may then write

$$T_{(\rho)}(q^2)=-\frac{g^2_{\rho qq}(q^2)}{q^2-m_\rho^2+im_\rho\Gamma_\rho(q^2)}, \tag{2.5}$$

where

$$m_\rho\Gamma_\rho(q^2)=g^2_{\rho qq}(q^2)\mathrm{Im}\,\hat{K}_{(\rho)}(q^2). \tag{2.6}$$

For this work we only consider the region $q^2\leqslant 0$. Therefore, $\hat{K}_{(\rho)}(q^2)$ will be real in our study. Values for $g_{\rho qq}(q^2)$ are obtained when equating the $T_{(\rho)}(q^2)$ of Eqs. (2.4) and (2.5).

In an analogous fashion, we may define

$$T_{(\omega)}(q^2)=-\frac{g^2_{\omega qq}(q^2)}{q^2-m_\omega^2+im_\omega\Gamma_\omega(q^2)}. \tag{2.7}$$

We have calculated $g_{\omega qq}(q^2)$ and $g_{\rho qq}(q^2)$ in an earlier work [8]. Values of $g_{\rho qq}(q^2)$ and $g_{\omega qq}(q^2)$ obtained there are presented in Table I. For that analysis we put $m_\rho=0.77$ GeV and $m_\omega=0.783$ GeV. A confining field was used of the form $V^C(r)=\kappa re^{-\mu r}$, where $\kappa=0.22$ GeV^2. (The parameter μ was introduced to soften the momentum-space singularities of the potential so as to facilitate the numerical analysis. We chose $\mu=0.050$ GeV.) The value of $g_{\rho qq}(m_\rho^2)$ obtained in Ref. [8] was used to calculate the rho-pion coupling constant, $g_{\rho\pi\pi}(m_\rho^2)$, and a good value was obtained [$g_{\rho\pi\pi}(m_\rho^2)=5.90$]. The coupling constants $g_{\rho qq}(m_\omega^2)$ and $g_{\omega qq}(m_\omega^2)$ were used in the calculation of the matrix element that describes rho-omega mixing $\theta(m_\omega^2)=\langle\omega|H_{\mathrm{SB}}|\rho^0\rangle$ [9]. We found a quite satisfactory value for $\theta(m_\omega^2)$ in Ref. [9]. These results lead us to believe that the momentum-space bosoniza-

tion scheme is working well, with respect to the calculation of the meson-quark coupling constants.

III. ELECTROMAGNETIC FORM FACTORS OF THE NUCLEON

In this section we review a number of well-known relations, with the aim of providing a phenomenological representation of the isoscalar and isovector form factors of the nucleon. We recall that proton and neutron form factors may be defined, with $e>0$,

$$\langle \vec{p}',s',\tau'=1/2|J^{\mu}_{\rm em}(0)|\vec{p},s,\tau=1/2\rangle = e\overline{u(\vec{p}',s')}\left[\gamma^{\mu}F_1^p(q^2)+\frac{i\sigma^{\mu\nu}}{2m_N}q_{\nu}F_2^p(q^2)\right]u(\vec{p},s), \quad (3.1)$$

$$\langle \vec{p}',s',\tau'=-1/2|J^{\mu}_{\rm em}(0)|\vec{p},s,\tau=-1/2\rangle = e\overline{u(\vec{p}',s')}\left[\gamma^{\mu}F_1^n(q^2)+\frac{i\sigma^{\mu\nu}}{2m_N}q_{\nu}F_2^n(q^2)\right]u(\vec{p},s). \quad (3.2)$$

Here $\vec{p}'=\vec{p}+\vec{q}$.

One further defines electric and magnetic form factors

$$G_E^p(q^2)=F_1^p(q^2)+\frac{q^2}{4m_N^2}F_2^p(q^2), \quad (3.3)$$

$$G_M^p(q^2)=F_1^p(q^2)+F_2^p(q^2), \quad (3.4)$$

$$G_E^n(q^2)=F_1^n(q^2)+\frac{q^2}{4m_N^2}F_2^n(q^2), \quad (3.5)$$

and

$$G_M^n(q^2)=F_1^n(q^2)+F_2^n(q^2). \quad (3.6)$$

We also put

$$F_1^p(q^2)=F_1^S(q^2)+F_1^V(q^2), \quad (3.7)$$

$$F_2^p(q^2)=F_2^S(q^2)+F_2^V(q^2), \quad (3.8)$$

$$F_1^n(q^2)=F_1^S(q^2)-F_2^V(q^2), \quad (3.9)$$

and

$$F_2^n(q^2)=F_2^S(q^2)-F_2^V(q^2). \quad (3.10)$$

We then solve for the isoscalar and isovector form factors

$$F_1^S(q^2)=\frac{G_E^p(q^2)+G_E^n(q^2)-(q^2/4m_N^2)[G_M^p(q^2)+G_M^n(q^2)]}{2(1-q^2/4m_N^2)}, \quad (3.11)$$

$$F_2^S(q^2)=\frac{[G_M^p(q^2)+G_M^n(q^2)]-[G_E^p(q^2)+G_E^n(q^2)]}{2(1-q^2/4m_N^2)}, \quad (3.12)$$

$$F_1^V(q^2)=\frac{[G_E^p(q^2)-G_E^n(q^2)]-(q^2/4m_N^2)[G_M^p(q^2)-G_M^n(q^2)]}{2(1-q^2/4m_N^2)}, \quad (3.13)$$

and

$$F_2^V(q^2)=\frac{[G_M^p(q^2)-G_M^n(q^2)]-[G_E^p(q^2)-G_E^n(q^2)]}{2(1-q^2/4m_N^2)}. \quad (3.14)$$

We remark that $F_1^S(0)=0.5$, $F_2^S(0)=-0.06$, $F_1^V(0)=0.5$, and $F_2^V(0)=1.85$. For the range of momentum of interest to us, we may use the dipole forms (with q^2 in GeV^2 units),

$$G_E^p(q^2)=\frac{1}{(1-q^2/0.71)^2}, \quad (3.15)$$

$$G_M^p(q^2)=\mu_p G_E^p(q^2), \quad (3.16)$$

$$G_M^n(q^2)=\mu_n G_E^p(q^2). \quad (3.17)$$

Here, $\mu_p=2.79$, $\mu_n=-1.91$, and $G_E^n(q^2)\simeq 0$. Use of Eqs. (3.15)–(3.17) in Eqs. (3.11)–(3.14) provides a phenomenological representation of the isoscalar and isovector form factors. We will describe a procedure for obtaining theoretical values for $F_1^S(q^2)$ and $F_2^V(q^2)$ in the next section.

IV. THE VECTOR-MESON-DOMINANCE MODEL FOR THE NUCLEON ELECTROMAGNETIC FORM FACTORS

It is well known that hadron electromagnetic form factors may be calculated in some form of the vector-meson-dominance (VMD) model. (Indeed, the VMD model provides a remarkably accurate representation of the pion form factor for both timelike and spacelike values of q^2 [10].) Here, we will develop a version of the VMD model for the nucleon electromagnetic form factors that will provide some information needed in the calculation of rho and omega exchange in our study of the nucleon-nucleon interaction.

We will not use the bag model in our analysis; however, we do have in mind a picture of the nucleon as a valence-quark ''core'' strongly coupled to surrounding meson fields. From this point of view, we may consider the processes shown in Fig. 2. There the wavy line denotes a photon, the

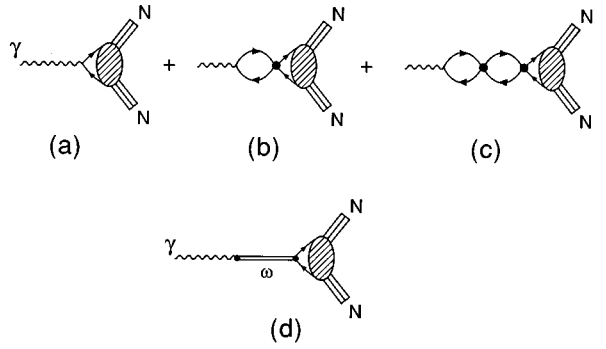

FIG. 2. (a) Here the wavy line represents a photon of momentum q. The lines with arrows denote quarks, while the crosshatched area represents a nucleon ''core'' that is ''dressed'' by various mesons ($\rho,\omega,\ldots$). (b) Here the solid dot denotes a coupling constant of the extended NJL model (G_ρ or G_ω). (c) Here we represent the development of the bubble string of the extended NJL model. The bubble string may be replaced by a meson propagator through the use of the relation $G_\rho/\{1-G_\rho[\hat{J}_{(\rho)}(q^2)+\hat{K}_{(\rho)}(q^2)]\} = -g^2_{\rho qq}(q^2)/[q^2-m^2_\rho]$ in the case of the rho meson, for example. (d) Via bosonization, one may introduce the omega propagator, which is represented by a double line in the figure. At the photon-meson vertex, one has a factor $m^2_\omega/g^\omega(q^2)$, where $g^\omega(q^2)$ is the momentum-dependent meson decay constant of the omega meson.

single lines are quarks and the crosshatched area represents the ''valence-quark core.'' In Fig. 2(a) the photon is absorbed by a quark in the core. The process shown in Fig. 2(a) gives rise to an isoscalar amplitude

$$A^\mu(p,p') = \frac{e}{2}\,\overline{u(\vec{p}',s')} \times\left[\gamma^\mu f_1^S(q^2)+\frac{i\sigma^{\mu\nu}}{2m_N}\,q_\nu f_2^S(q^2)\right]u(\vec{p},s), \tag{4.1}$$

where $f_1^S(q^2)$ and $f_2^S(q^2)$ are form factors of the core. In Figs. 2(a) and 2(b), we see the photon being absorbed, with subsequent rescattering of the quark-antiquark pair. (Note that we do not show the confinement vertex in these figures to avoid excessive complexity in the figure.) Inclusion of the full series of $q\overline{q}$ ''bubbles,'' as shown in Figs. 2(a)–2(c), etc., yields the amplitude in the omega channel ($J=1^-$, $I=0$)

$$B^\mu_{(\omega)}(p',p) = \frac{e}{2}\,\frac{1}{1-G_\omega[\hat{J}_{(\omega)}(q^2)+\hat{K}_{(\omega)}(q^2)]}\,\overline{u(\vec{p}',s')} \times\left[\gamma^\mu f_1^S(q^2)+\frac{i\sigma^{\mu\nu}}{2m_N}\,q_\nu f_2^S(q^2)\right]u(\vec{p},s). \tag{4.2}$$

From this form we may identify the VMD result by using our bosonization relations. [See Eqs. (2.4), (2.5), and (2.7).] We find

$$B^\mu_{(\omega)}(p',p) = \frac{e}{2}\,\frac{1}{G_\omega}\,\frac{g^2_{\omega qq}(q^2)}{m^2_\omega-q^2}\,\overline{u(p',s')} \times\left[\gamma^\mu f_1^S(q^2)+\frac{i\sigma^{\mu\nu}q_\nu}{2m_N}\,f_2^S(q^2)\right]u(\vec{p},s). \tag{4.3}$$

This may be put in a somewhat more familiar form by defining a meson decay constant $g^\omega(q^2)$ [10]:

$$\frac{m^2_\omega}{g^\omega(q^2)} = \frac{g_{\omega qq}(q^2)}{6G_\omega}. \tag{4.4}$$

Thus

$$B^\mu_{(\omega)}(p',p) = e\left(\frac{m^2_\omega}{g^\omega(q^2)}\right)\,\frac{1}{m^2_\omega-q^2}\,g_{\omega qq}(q^2)\overline{u(\vec{p}',s')} \times\left[\gamma^\mu f_1^S(q^2)+\frac{i\sigma^{\mu\nu}}{2m_N}\,q_\nu f_2^S(q^2)\right]u(\vec{p},s). \tag{4.5}$$

Thus, we may identify isoscalar form factors of the nucleon

$$F_1^S(q^2) = \frac{1}{6G_\omega}\,\frac{g^2_{\omega qq}(q^2)}{m^2_\omega-q^2}\,f_1^S(q^2), \tag{4.6}$$

$$F_2^S(q^2) = \frac{1}{6G_\omega}\,\frac{g^2_{\omega qq}(q^2)}{m^2_\omega-q^2}\,f_2^S(q^2). \tag{4.7}$$

We can define $f_1^S(0)=3$ and require that $f_2^S(0)=-0.36$. [Since $f_2^S(0)$ is quite small, we will neglect it at this point.] We may use $G_\omega=24.3$ GeV^{-2}, $m_\omega=0.783$ GeV, and $g_{\omega qq}(0)=3.86$, and find $F_1^S(0)=0.5$. Note that $g^2_{\omega qq}(0)/(m^2_\omega G_\omega)=1$ in a gauge-invariant formalism.

For the isovector form factors, entirely similar considerations allow us to write

$$F_1^V(q^2) = \frac{1}{2G_\rho}\,\frac{g^2_{\rho qq}(q^2)}{m^2_\rho-q^2}\,f_1^V(q^2), \tag{4.8}$$

$$F_2^V(q^2) = \frac{1}{2G_\rho}\,\frac{g^2_{\rho qq}(q^2)}{m^2_\rho-q^2}\,f_2^V(q^2). \tag{4.9}$$

Here, we require $f_1^V(0)=1$ and $f_2^V(0)=3.70$, so that $F_1^V(0)=0.5$ and $F_2^V(0)=1.85$. Note that $g^2_{\rho qq}(0)/(m^2_\rho G_\rho)=1$ with $G_\rho=22.6$ GeV^{-2}.

We have seen in past work that, if one uses a relativistic version of the SU(6) quark-model wave functions of the nucleon, it is quite easy to fit the $q^2=0$ values of the nucleon form factors in what may be considered to be a pure ''core'' model [11]. That is, in Ref. [11], we did not use the VMD model, nor did we consider the contribution of the ''meson cloud.'' The success of that analysis was based on the fact that, if one calculates the matrix element of the isoscalar current, $j^\mu_S(x)=\overline{q(x)}\,\gamma^\mu q(x)$, between nucleon states, the resulting value of $f_2^S(0)$ is quite small. On the other hand, if one calculates the matrix element of the isovector current,

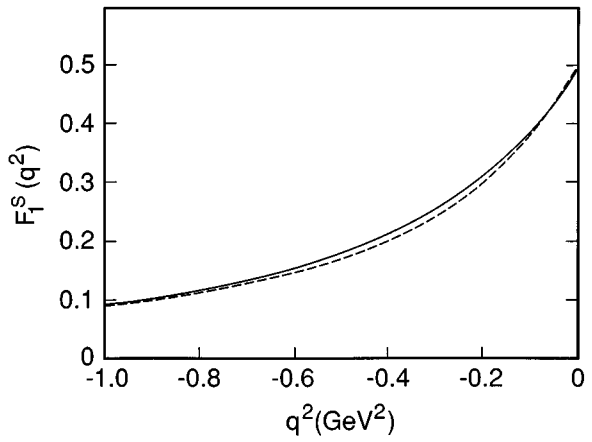

FIG. 3. Values of $F_1^S(q^2)$ are shown. The phenomenological values are given by the solid line, while the result of our fit using the VMD model is represented by the dashed line. Here $\lambda_1^S=0.745$ GeV. [See Eq. (4.12).]

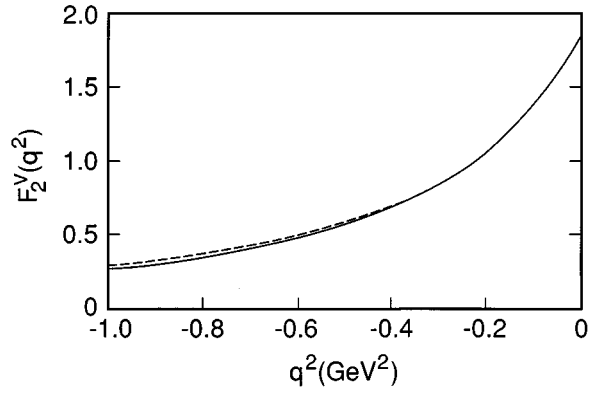

FIG. 4. Values of $F_2^S(q^2)$ are shown. The phenomenological values are given by the solid line, while the dashed line shows the result of the VMD model with $\lambda_2^V=0.70$ GeV. [See Eq. (4.11).]

$j_V^\mu(x)=\overline{q(x)}\gamma^\mu\tau_3 q(x)$, a large value of $f_2^V(0)$ is obtained. Indeed, the moments of the neutron and proton were very well fitted by the simple ''core'' model of Ref. [11]. However, in the present work we have used a VMD model and a nucleon ''core'' to facilitate our study of the nucleon-nucleon force due to vector-meson exchange.

The purpose of the foregoing analysis was to find some information concerning the core form factors. To that end, we put

$$f_1^V(q^2)=\frac{(\lambda_1^V)^2}{(\lambda_1^V)^2-q^2}, \tag{4.10}$$

$$f_2^V(q^2)=3.70\,\frac{(\lambda_2^V)^2}{(\lambda_2^V)^2-q^2}, \tag{4.11}$$

$$f_1^S(q^2)=3\,\frac{(\lambda_1^S)^2}{(\lambda_1^S)^2-q^2}, \tag{4.12}$$

$$f_2^S(q^2)=-0.36\,\frac{(\lambda_2^S)^2}{(\lambda_2^S)^2-q^2}. \tag{4.13}$$

At this point, we may find values of the various λ's by using the phenomenological values of F_1^S, F_2^S, F_1^V, and F_2^V given in Sec. III. We will concentrate on $F_1^S(q^2)$ and $F_2^V(q^2)$, since these form factors appear in the most important components of the nucleon-nucleon interaction that arise from vector-meson exchange. In Fig. 3 we show a fit to $F_1^S(q^2)$ obtained with $\lambda_1^S=0.745$ GeV and in Fig. 4 we show a fit to $F_2^V(q^2)$ obtained with $\lambda_2^V=0.70$ GeV. (If we convert these values of λ to a ''core radius'' by using the formula $R=\sqrt{6}/\lambda$, we find $R_\rho\simeq 0.69$ fm and $R_\omega\simeq 0.65$ fm. These values represent about 80% of the value of the electromagnetic radius of the nucleon.)

V. VECTOR-MESON EXCHANGE IN THE OBE MODEL

The one-boson-exchange model provides a particularly simple representation of the nucleon-nucleon interaction [1]. One characteristic of the model is the inclusion of a vertex cutoff at each meson-nucleon vertex. For the monopole form of the vertex cutoff, we have, for meson i,

$$\mathcal{F}_i^{\rm OBE}(q^2)=\frac{\Lambda_i^2-m_i^2}{\Lambda_i^2-q^2} \tag{5.1}$$

at each vertex. For example, for omega exchange, one has an amplitude

$$f_{(\omega)}^{\rm OBE}(q^2)=\frac{g_{\omega NN}^2}{4\pi}\left(\frac{\Lambda_\omega^2-m_\omega^2}{\Lambda_\omega^2-q^2}\right)^2\frac{1}{m_\omega^2-q^2}. \tag{5.2}$$

Here, $g_{\omega NN}$ is the omega-nucleon coupling constant as defined in Ref. [1]. We have included a factor of $(1/4\pi)$ in Eq. (5.2), since the value of the coupling constant is usually given by specifying the value of $g^2/4\pi$. For example, we have $g_{\omega NN}^2/4\pi=20.0$ and $\Lambda_\omega=1.5$ GeV as typical values in the OBE model [1]. From these values, we have $f_{(\omega)}^{\rm OBE}=17.26$ GeV^{-2}, if we use the definition of $f_{(\omega)}^{\rm OBE}(q^2)$ given in Eq. (5.2).

To calculate the corresponding amplitude in the extended NJL model, we consider the diagrams of Fig. 5. Note that to obtain an expression similar to that of the OBE model, we may consider the interaction of the valence quark ''cores'' that were introduced in the last section. For example, we may write, for omega exchange,

$$\begin{aligned}\Gamma_{\rm NJL}^\mu=&\overline{u(\vec{p}_2-\vec{q},s_2')}\left[\gamma^\mu f_1^S(q^2)-\frac{i\sigma^{\mu\nu}}{2m_N}q_\nu f_2^S(q^2)\right]\\&\times u(\vec{p}_2,s_2)\,\frac{G_\omega}{1-G_\omega\hat{J}_{(\omega)}(q^2)}\\&\times\overline{u(\vec{p}_1+\vec{q},s_1')}\left[\gamma^\mu f_1^S(q^2)+\frac{i\sigma^{\mu\nu}}{2m}q_\nu f_2^S(q^2)\right]\\&\times u(\vec{p}_1,s_1).\end{aligned} \tag{5.3}$$

We now use our basic bosonization relations to extract the amplitude proportion to $[f_1^S(q^2)]^2$. We again insert a factor of $(1/4\pi)$ and write

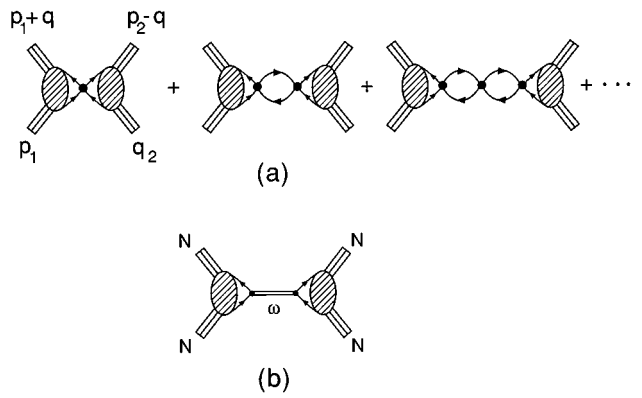

FIG. 5. (a) Diagrams that are considered when using the extended NJL model to calculate the meson-exchange between two nucleon core states. The solid dot represents either G_ρ or G_ω. The ''bubble string'' may be summed by using the relation $G_\omega/[1-G_\omega \hat{J}_{(\omega)}(q^2)]=-g^2_{\omega qq}(q^2)/(q^2-m^2_\omega)$ in the case of the isoscalar qq channel, for example. (b) The omega propagator is shown as a double line. The small solid dots denote factors of $g_{\omega qq}(q^2)$.

$$f^{\rm NJL}_{(\omega)}(q^2)=\frac{1}{4\pi}\,\frac{g^2_{\omega qq}(q^2)}{m^2_\omega-q^2}\,[f^S_1(q^2)]^2 \tag{5.4}$$

$$=\frac{1}{4\pi}\,t^{(\omega)}_{qq}(q^2)\left(\frac{(\lambda^S_1)^2}{(\lambda^S_1)^2-q^2}\right)^2[f^S_1(0)]^2, \tag{5.5}$$

where we have put $t^{(\omega)}_{qq}(q^2)=g^2_{\omega qq}(q^2)/(m^2_\omega-q^2)$ and made use of Eq. (4.12). With $\lambda^S_1=0.745$ GeV, $g_{\omega qq}(0)=3.86$ (see Table I) and $f^S_1(0)=3.0$, we obtain $f^{\rm NJL}_{(\omega)}(0)=17.4$ GeV^{-2}, which is close to the value $f^{\rm OBE}_{(\omega)}(0)=17.3$ GeV^{-2} calculated above. The functions $f^{\rm NJL}_{(\omega)}(q^2)$ and $f^{\rm OBE}_{(\omega)}(q^2)$ are compared in Fig. 6. We see that $f^{\rm NJL}_{(\omega)}(q^2)$ falls off more quickly than $f^{\rm OBE}_{(\omega)}(q^2)$ as $-q^2$ is increased.

We now turn to a consideration of rho exchange. Here we will concentrate on the tensor component of the force. In the OBE model, we consider the amplitude

$$f^{\rm OBE}_{(\rho)}(q^2)=\frac{f^2_{\rho NN}}{4\pi}\left(\frac{\Lambda^2_\rho-m^2_\rho}{\Lambda^2_\rho-q^2}\right)^2\frac{1}{m^2_\rho-q^2}, \tag{5.6}$$

where, in the OBE model, $f_{\rho NN}$ is related to $g_{\rho NN}$ by $f_{\rho NN}/g_{\rho NN}=6.1$ [1]. The coupling constants, $g_{\rho NN}$ and $f_{\rho NN}$, are used to parametrize the form of the meson-nucleon vertex in the OBE model. For example, the vertex for rho-nucleon coupling is [1]

$$\Gamma^\mu_{\rm OBE}=\overline{u(\vec{p}+\vec{q},s')}\left[g_{\rho NN}\gamma^\mu+f_{\rho NN}\,\frac{i\sigma^{\mu\nu}q_\nu}{2m_N}\right]$$
$$\times u(\vec{p},s)\langle\tau'|\tau_3|\tau\rangle\left(\frac{\Lambda^2_\rho-m^2_\rho}{\Lambda^2_\rho-q^2}\right). \tag{5.7}$$

Here, we see that, in the case of the OBE model, the same value of Λ_ρ is used in the central and the tensor term. We have $g^2_{\rho NN}/4\pi=0.99$ and $\Lambda_\rho=1.3$ GeV as typical values in the OBE model. (See Table A.2 of Ref. [1].) Thus, $f^2_{\rho NN}/4\pi=36.8$ in the OBE model and, from Eq. (5.6), we find $f^{\rm OBE}_{(\rho)}(0)=26.2$ GeV^{-2}.

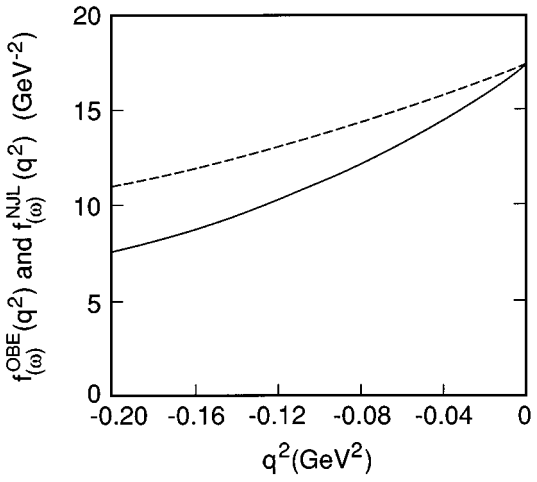

FIG. 6. The figure shows values of $f^{\rm OBE}_{(\omega)}(q^2)$ (dashed line) and $f^{\rm NJL}_{(\omega)}(q^2)$ (solid line). [See Eqs. (5.2) and (5.4).]

The NJL amplitude is obtained by considering an expression analogous to Eq. (5.3). In Eq. (5.8) we have not written the isospin factors, for simplicity. Thus,

$$\Gamma^\mu_{\rm NJL}=\overline{u(\vec{p}_2-\vec{q},s'_2)}\left[\gamma^\mu f^V_1(q^2)-\frac{i\sigma^{\mu\nu}q_\nu}{2m_N}\,f^V_2(q^2)\right]$$
$$\times u(\vec{p}_2,s_2)\,\frac{G_\rho}{1-G_\rho[\hat{J}_{(\rho)}(q^2)+\hat{K}_{(\rho)}(q^2)]}$$
$$\times\overline{u(\vec{p}_1+\vec{q},s'_1)}\left[\gamma^\mu f^V_1(q^2)+\frac{i\sigma^{\mu\beta}q_\beta}{2m_N}\,f^V_2(q^2)\right]$$
$$\times u(\vec{p}_1,s_1), \tag{5.8}$$

$$f^{\rm NJL}_{(\rho)}(q^2)=\frac{1}{4\pi}\,\frac{G_\rho}{1-G_\rho[\hat{J}_{(\rho)}(q^2)+\hat{K}_{(\rho)}(q^2)]}\,[f^V_2(q^2)]^2 \tag{5.9}$$

$$=\frac{1}{4\pi}\,\frac{g^2_{\rho qq}(q^2)}{m^2_\rho-q^2}\,[f^V_2(q^2)]^2 \tag{5.10}$$

$$=\frac{1}{4\pi}\,t^{(\rho)}_{qq}(q^2)\left(\frac{(\lambda^V_2)^2}{(\lambda^V_2)^2-q^2}\right)^2[f^V_2(0)]^2. \tag{5.11}$$

Noting that $g_{\rho qq}(0)=3.66$, $f^V_2(0)=3.70$, and $m_\rho=0.77$ GeV, we find $f^{\rm NJL}_{(\rho)}(0)=24.6$ GeV^{-2}, which is 94% of the corresponding OBE result given above: $f^{\rm OBE}_{(\rho)}(0)=26.2$ GeV^{-2}. (See Fig. 7 and Table II.)

VI. DISCUSSION

It is worth noting that, if we had calculated the magnitude of the NJL amplitude using the values of the meson-quark coupling constants at $q^2=m^2_\omega$, or $q^2=m^2_\rho$, we would have found only about 60% of the value of the OBE amplitude at

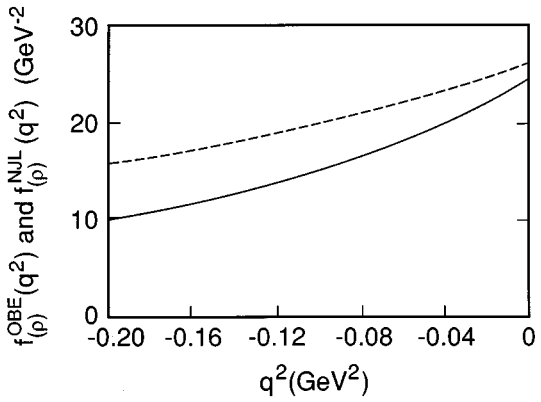

FIG. 7. The figure shows values of $f^{\mathrm{OBE}}_{(\rho)}(q^2)$ (dashed line) and $f^{\mathrm{NJL}}_{(\rho)}(q^2)$ (solid line). [See Eqs. (5.6) and (5.11).]

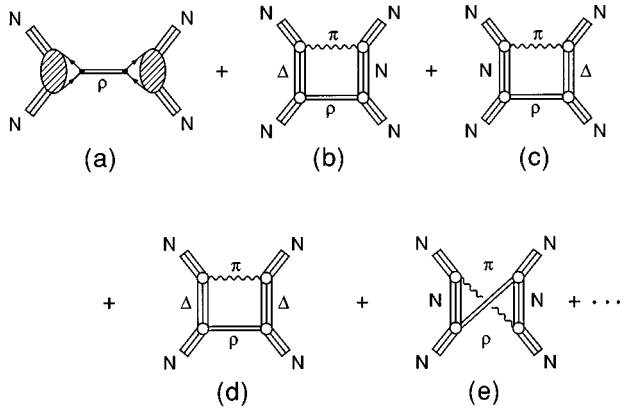

FIG. 8. Processes that contribute to t-channel exchange with the quantum numbers of the rho. (a) The model for $f^{\mathrm{NJL}}_{(\rho)}(q^2)$ used in this work is shown. Here the double line is a rho propagator and the small filled dots represent rho-quark coupling constants. (b)–(e) Various processes involving intermediate states of a delta and a nucleon (or two deltas) that can contribute to t-channel exchange with the quantum numbers of the rho.

$q^2=0$. That is, the momentum dependence of $g_{\rho qq}(q^2)$ and $g_{\omega qq}(q^2)$ is quite important, since $[g_{\rho qq}(m^2_\rho)/g_{\rho qq}(0)]^2$ and $[g_{\omega qq}(m^2_\omega)/g_{\omega qq}(0)]^2$ are both equal to approximately 0.6. (See Table I.)

We need not expect perfect agreement when comparing OBE and NJL amplitudes, since, for the nucleon-nucleon scattering problem, there are many diagrams (corresponding to shorter-range forces) that we have not considered. Some such diagrams are shown in Figs. 8(b)–8(e). The fact that our amplitudes fall off more rapidly with q^2 than the OBE amplitudes may indicate that the shorter-range processes shown in Figs. 8(b)–8(e) are important for t-channel exchange processes with the quantum numbers of the omega and the rho mesons.

In recent years there has been some interest in studying nucleon-nucleon scattering in models that exhibit chiral symmetry at the meson-nucleon level [12]. In an earlier work [13] we studied various two-pion exchange diagrams that arose in a chiral model of the pion-nucleon interaction [14]. We calculated two-nucleon-irreducible amplitudes, since our goal was to study a potential that could be iterated in a Bethe-Salpeter equation. We also limited our considerations to the isospin zero potentials. The two-pion-exchange diagrams were classed as two-point loop diagrams, three-point loop diagrams, box diagrams, and crossed-box diagrams. (See Fig. 2 of Ref. [13].) The results were sensitive to a cutoff, Λ, that was used to make the various two-pion-exchange diagrams finite. (Also, when calculating the *irreducible* amplitudes, the result depends upon whether one uses pseudoscalar or pseudovector coupling of the pion to the nucleon.)

TABLE II. Parameters of the OBE model for rho and omega exchange and those calculated in this work. For the OBE parameters, see Table A.2 of Ref. [1]. Here $\kappa=f_{\rho NN}/g_{\rho NN}$.

	OBE	NJL (this work)
$\frac{g^2_{\rho NN}}{4\pi}$	0.99	2.52
$\frac{f^2_{\rho NN}}{4\pi}$	36.8	34.6
κ	6.1	3.7
$\frac{g^2_{\omega NN}}{4\pi}$	20.0	20.0

In Ref. [13] we presented a tensor decomposition of the interaction. The resulting potentials had quantum numbers that allowed for their classification as scalar, vector, pseudovector, axial-vector and tensor-exchange potentials. The (isoscalar) vector-exchange potential (that has its origin in two-pion exchange) acts in the same channel as the omega-exchange potential considered in this work. For the irreducible interaction, with pseudovector pion-nucleon coupling, the contribution to the isoscalar vector interaction was very small. (See Figs. 7 and 8 of Ref. [13].) For pseudoscalar coupling of the pion to the nucleon, the irreducible potential corresponding to isoscalar vector exchange was repulsive. This two-pion exchange potential corresponded to an amplitude, at $q^2=0$, that was about 4–6% of the value of $f^{\mathrm{NJL}}_{\omega}(0)$ calculated in the present work. (See Figs. 5 and 6 of Ref. [13].) These results suggest that those corrections to the model for vector exchange considered in the present work, that would arise from the implementation of chiral symmetry at the meson-nucleon level, are small. (As noted in Ref. [13], if we calculated the two-nucleon-*reducible* amplitudes for two-pion exchange, the results are the same for the pseudoscalar and the pseudovector pion-nucleon coupling schemes.)

Some further support for the application of the NJL model in the calculation of the nucleon-nucleon interaction comes from our study of pion exchange. In Ref. [3] we considered the amplitude

$$h^{\mathrm{NJL}}_{\pi}(q^2)=\frac{t^{(\pi)}_{qq}(q^2)}{t^{(\pi)}_{qq}(0)}\left(\frac{\lambda^2_\pi}{\lambda^2_\pi-q^2}\right)^2, \tag{6.1}$$

where $t^{(\pi)}_{qq}(q^2)$ is the T matrix for quark-quark scattering with t-channel pion exchange. [Note that $h^{\mathrm{NJL}}_{\pi}(0)=1$.] Here λ_π parametrizes the momentum dependence of the pion-nucleon vertex. Since $t^{(\pi)}_{qq}(q^2)$ was fixed by the NJL model, we only had the single parameter, λ_π, to adjust when fitting the corresponding OBE amplitude,

$$h_\pi^{\rm OBE}(q^2) = -\left(\frac{\Lambda_\pi^2}{\Lambda_\pi^2 - q^2}\right)^2 \frac{m_\pi^2}{q^2 - m_\pi^2}, \qquad (6.2)$$

where $\Lambda_\pi = 1.3$ GeV [1]. We found that the choice of $\Lambda_\pi = 0.80$ GeV put $h_{\pi_n}^{\rm NJL}(q^2)$ and $h_\pi^{\rm OBE}(q^2)$ in excellent agreement for spacelike q^2 out to $q^2 = -2.0$ GeV^2. Recently, it was found that $\lambda_\pi \simeq 0.8$ GeV in an application of QCD sum rules in the calculation of the momentum dependence of the pion-nucleon vertex [15]. That result lends some further support for the application of our extended NJL model in the calculation of the nucleon-nucleon interaction.

ACKNOWLEDGMENTS

This work was supported in part by a grant from the National Science Foundation and by the PSC-CUNY Faculty Award Program of the City University of New York.

[1] R. Machleidt, in *Advances in Nuclear Physics*, edited by J. W. Negele and E. Vogt (Plenum, New York, 1989), Vol. 19.
[2] L. S. Celenza and C. M. Shakin, *Relativistic Nuclear Physics: Theories of Structure and Scattering* (World Scientific, Singapore, 1986).
[3] C. M. Shakin, Wei-Dong Sun, and J. Szweda, Phys. Rev. D **52**, 3353 (1995).
[4] Shun-fu Gao, L. S. Celenza, C. M. Shakin, Wei-Dong Sun, and J. Szweda, Phys. Rev. C **53**, 1936 (1996).
[5] L. S. Celenza, C. M. Shakin, Wei-Dong Sun, J. Szweda, and Xiquan Zhu, Int. J. Mod. Phys. E **2**, 603 (1993). In this reference Re $C(P^2)$ should be replaced by Re $C(P^2) + \hat{J}_S(P^2)$.
[6] L. S. Celenza, C. M. Shakin, Wei-Dong Sun, J. Szweda, and Xiquan Zhu, Phys. Rev. D **51**, 3638 (1995).
[7] L. S. Celenza, C. M. Shakin, Wei-Dong Sun, J. Szweda, and Xiquan Zhu, Ann. Phys. (N.Y.) **241**, 1 (1995).
[8] L. S. Celenza, C. M. Shakin, Wei-Dong Sun, and J. Szweda, Brooklyn College Report No. BCCNT 95/032/245R1, 1995, unpublished.
[9] Shun-fu Gao, C. M. Shakin, and Wei-Dong Sun, Phys. Rev. C **53**, 1374 (1996).
[10] A derivation of the vector-meson-dominance model based upon the momentum-space bosonization of the extended NJL model is given in C. M. Shakin and Wei-Dong Sun, Brooklyn College Report No. BCCNT 95/101/251, 1995; R. Friedrich and H. Reinhardt, Nucl. Phys. **A594**, 406 (1995).
[11] L. S. Celenza, A. Rosenthal, and C. M. Shakin, Phys. Rev. C **31**, 212 (1985).
[12] C. Ordonez, L. Ray, and U. van Kolck, Phys. Rev. Lett. **72**, 1982 (1994).
[13] L. S. Celenza, A. Pantziris, and C. M. Shakin, Phys. Rev. C **46**, 2213 (1992).
[14] K. Kang and A. Pantziris, Phys. Rev. D **43**, 241 (1991).
[15] T. Meissner, Phys. Rev. C **52**, 3386 (1995).